HHS Public Access

Author manuscript

Nat Neurosci. Author manuscript; available in PMC 2013 November 10.

Published in final edited form as:

Nat Neurosci. 2013 May ; 16(5): 529–531. doi:10.1038/nn.3368.

Activation of transposable elements during aging and neuronal decline in *Drosophila*

W. Li[1,2,3], **L. Prazak**[1,3], **N. Chatterjee**[1], **S Grüninger**[4,5], **L. Krug**[5], **D. Theodorou**[6], and **J. Dubnau**[1,5,7]

[1]Cold Spring Harbor Laboratory, Cold Spring Harbor, NY 11724, USA [2]Graduate Program in Molecular and Cellular Biology, Stony Brook University, Stony Brook, NY 11794, USA [4]Institute of Neuroinformatics, University of Zurich, 8057 Zurich, Switzerland [5]Watson School of Biological Sciences, Cold Spring Harbor Laboratory [6]Magistère de Génétique Graduate Program at Université Paris Diderot, Sorbonne Paris Cité

Abstract

We report the surprising finding that several transposable elements are highly active in *Drosophila* brain during normal aging. We also show that mutations in *Drosophila Argonaute 2* (*dAgo2*) exhibit exacerbated transposon expression in brain, progressive and age-dependent memory impairment and shortened lifespan. These findings suggest that transposon activation may contribute to age-dependent loss of neuronal function.

Transposable elements (TEs) are highly abundant mobile genetic elements that constitute a large fraction of most eukaryotic genomes [1,2]. Retrotransposons, which replicate through an RNA intermediate, represent approximately 40% and 30% of the human and *Drosophila* genomes respectively. Mounting evidence suggests that TEs can be active not only in the germline, but also in the brain. LINE-1 elements, for instance, are actively mobilized in normal mammalian brains during neurogenesis[3–5], leading to genetic heterogeneity, which in principle could have a functional role in neurophysiology. However, because TEs are capable of replicating and inserting into new positions in the genome, they represent a massive reservoir of potential genomic instability as well as RNA-level toxicity. In fact, TE activation has been correlated with several neurodegenerative disorders[6–13].

We examined TE expression in *Drosophila*, where it is feasible to manipulate the TE control mechanisms and to measure physiological effects on the nervous system. We first used

[7]Corresponding author. dubnau@cshl.edu.

[3]These authors contributed equally to this work and are listed alphabetically

Author Contributions:

W.L and L.P contributed equally. W.L, L.P and J. D conceived and designed the project and analyzed the experiments. The behavior experiments and western blots were performed by W.L. The QPCR and lifespan analyses were performed by L.P with assistance from W. L, C.S, L.K. and T.D. Imaging experiments were performed by L.P, N.C. and S.G. The manuscript was written by W.L, L.P. and J.D with comments from the other authors.

Competing interests: This work was funded in part by DART LLC via a research grant to J.Dubnau

Quantitative Real-Time PCR (QPCR) to measure levels of several TE transcripts in head tissues during normal aging by comparing transcript levels from 2–4-day old adult wild-type flies with that of ~14, ~21 and ~28-day old counterparts. Surprisingly, transcripts from *R2*, a LINE-like element and *gypsy*, an LTR element are dramatically elevated in aged relative to young animals (Fig. 1A). *R1*, a second LINE-like element also shows elevated expression with age (see below). Although we have not exhaustively examined expression of the TE families in the Drosophila genome, the age-dependent expression may impact certain TEs specifically because we do not see effects on *gypsy4* or *Zam* (data not shown). In addition to the effects on transcripts from *gypsy*, *R1* and *R2*, we detect age-dependent increase in expression of the *gypsy* membrane glycoprotein ENV, using immunohistochemical staining in whole mount brains (Fig. 1B). The ENV signal is most intense in the cortical regions that contain most of the cell bodies, but also is detected in neuropil, areas containing axons and dendrites (central brain projections shown in Fig 1B; see also individual confocal sections Figs 3B and S5B). This age-dependent de-repression of TEs is not due to loss of expression of either Dicer-2 or dAGO2, proteins required for TE silencing in somatic tissues [14] (Fig. S1).

To determine if expression of gypsy in older animals is associated with physical transposition, we designed a *"gypsy-TRAP"* reporter system to detect *de novo gypsy* integration events. We adapted an elegant reporter system that was previously established for detecting *gypsy* integration in the germline[15]. To achieve this, we expressed GAL80, which is an effective repressor of GAL4, under control of the ubiquitous *α-tubulin* promoter. In the presence of GAL80 protein, GAL4-mediated expression of GFP is effectively silenced. We placed a ~500bp fragment from the *ovo* regulatory region between the promoter and *GAL80* in order to attract *gypsy* insertional mutations (Fig. S2A). This fragment contains 5 Ovo binding sites to which the Ovo protein normally binds in its own regulatory region. In the germline, these Ovo binding sites are necessary and sufficient to attract *de novo gypsy* insertions[15]. In our reporter system, somatic integration of *gypsy* downstream of the promoter or within the *GAL80* transcription unit disrupts expression of GAL80, permitting activation of GFP by GAL4 (Fig. 2B).

We used this system to screen for *de novo gypsy* integration events in the brain by focusing on neurons of the mushroom body (MB) for which highly specific and strongly expressing *GAL4* lines exist. We used the *MB247 GAL4* line[16], which is known to label about 800 out of ~2000–2500 mushroom body Kenyon cell neurons per brain hemisphere (Fig. 2A). GAL80 expression from our "*gypsy-TRAP"* (*Tubp-OvoSite-GAL80)* transformant lines is sufficient to silence GFP (Figs. 2 and S2). In fact, we do not observe any labeled neurons in 2–4-day old animals containing this construct (0/26 brains from 2–4day old animals, Figs. 2B, 2C, S2 and Table S1). However, we observe sparse GFP-labeled MB Kenyon cells at later ages in each of two transformant lines containing "*gypsy-TRAP"* (*Tubp-OvoSite-GAL80),* often in multiple neurons (14/39 brains labeled from 28–35 day old animals, Figs. 2E, S2 and Table S1). This effect of age was statistically significant (Chi-square Analysis, $p<0.01$). The labeling appears to be stochastic because we see both intra and inter-hemisphere variation. The accumulation of GFP positive neurons also requires the 5 Ovo binding sites, as is true for gypsy insertions in the germline, because we do not observe any

GFP labeled cells in control transformant lines containing a *"gypsy-TRAP"* with an ovo fragment in which the binding sites are mutated (*Tubp-MutatedOvoSite-GAL80)* (Figs. 2B; S2; Table S1; Chi-square Analysis, $p<0.001$). Our results using this reporter system strongly support the conclusion that *gypsy* not only is expressed in neurons of aging animals, but also is actively mobile in an age dependent manner.

We next used genetic manipulations of *dAgo2* to create a situation in which transposons are unleashed prematurely in young animals. In both animals and plants, TE control is mediated by Argonaute proteins guided by small regulatory RNAs[14]. Germline tissues are protected against TEs by the concerted action of Argonaute proteins of the PIWI clade and their small RNA partners, the piRNAs[14]. While control of TEs in somatic tissues in *Drosophila* is dependent on dAGO2 guided by endogenous small interfering RNAs, a different Argonaute protein in flies, dAGO1, preferentially loads the microRNAs that target cellular mRNAs, but has no known impact on TEs. Therefore, using *dAgo2* mutants, we can create a condition in which we selectively disrupt the somatic TE control mechanism.

Although *dAgo2* mutants have been shown to exhibit elevated TE expression in somatic tissue, the phenotypic consequences of such mutations on aging are not known. We found that transcripts from *R2* and *gypsy* are significantly elevated in head tissue of young $dAgo2^{414}$ and $dAgo2^{51B}$ mutant animals, as well as in trans-heterozygous $dAgo2^{414/51B}$ animals (Figs S4A and 3A). In addition, the age-dependent elevation of both *R2* and *gypsy* expression is accelerated in the *dAgo2* mutants such that transcript levels of both *R2* and *gypsy* in 2–4-day old mutant animals are comparable to that seen in ~28-day old wild type animals. At the protein level we observe an accelerated age dependent increase in ENV in *dAgo2* mutants (the $dAgo2^{414}$ and $dAgo2^{51B}$ hypomorphic alleles and the $dAgo2^{454}$ null allele) both in whole mount brains (Figs. 3B and S5B) and on western blots from adult heads (Figs. 3C and S5A). Furthermore, elevated expression of gypsy in *dAgo2* mutants also is associated with *de novo* insertions into the *ovo* locus, as detected by genomic PCR and sequencing (Fig. S3).

To investigate the correlation between age-dependent neuronal decline and TE activation, we used a robust and sensitive Pavlovian learning and memory assay that is well established in *Drosophila*[17]. We compared 24-hour LTM performance in animals that were trained when they were young (2–4-day) or trained when they were at an intermediate age (~20-day). *dAgo2* mutants already exhibit a partial reduction in memory at 2–4-days old (Figs. S4C, S4D, 3D), an effect which can be rescued by neuronal expression of a *dAgo2* transgene (Fig. S4E). The mild defect seen in young animals becomes dramatically worse in 20-day old adults (Fig. 3D). In contrast, wild-type animals trained at the ~20-days age exhibit normal robust levels of LTM that are equivalent to that seen in 2–4-day old wild type animals (Fig. 3D), only developing impairment at ~28-day of age (Fig. S7B).

We also examined the effects of *dAgo2* mutations on longevity and found that $dAgo2^{414}$, $dAgo2^{51B}$ and $dAgo2^{454}$ mutants exhibit significantly shorter lifespans than their wild type counterparts (Figs. 3E and S5C). This finding is consistent with reports that mutations in *Dicer-2*[18] and *loquacious*[19], other components of the somatic small RNA-dependent TE silencing pathway, also exhibit short lifespan. Although *dAgo2* mutants are susceptible to

exogenous viruses, viral infections do not contribute to the age-dependent decline in these mutants and do not cause the observed induction of transposons (Fig. S6).

TE activation in the germline is sufficient to cause sterility, at least in part by triggering Checkpoint kinase 2 (Chk2)-mediated DNA damage-induced apoptosis. In fact, disruption of Chk2 in the germline prevents cells from undergoing programmed cell death, which is sufficient to suppress TE dependent sterility[20]. To test whether DNA-damage leading to Chk2 signaling also contributs to age dependent mortality in wild type animals, we used an RNAi transgene to target *loki*, the *Drosophila* ortholog of *chk2*. Remarkably, we found that disrupting *loki* function exclusively in neurons by expressing the *lokiRNAi* under control of the pan-neuronal *elav-GAL4* can significantly delay mortality (Figs. S7A and 3F). This disruption of *loki* function also yields a modest but significant delay in age-dependent memory impairment (Fig. S7B and S7C). Although a causal role for TE activation and TE-induced DNA damage in age-related neuronal decline remains to be demonstrated, the effects with disruption of Chk2 signaling are at least consistent with this interpretation.

There is accumulating evidence that TEs actively mobilize in neurons[3,4]. This phenomenology has lead to the suggestion that regulated TE jumping provides a source of somatic mosaicism that may contribute to normal brain physiology, although such functional effects remain to be established. On the other hand, LINE, SINE and LTR elements are de-repressed in a variety of neurodegenerative diseases[6–13], suggesting the possibility that misregulation of TEs is detrimental. The results reported here, together with the above literature, suggest the novel hypothesis that TE activation with age or disease may contribute to neuronal decline.

ONLINE METHODS

Fly Stocks

The wild type flies utilized in this study were w^{1118} *(isoCJ1)*, a Canton-S derivative[21]. The *dAgo2* mutants and *UAS::dAgo2* transgenic strains were backcrossed to the above wild type strain for at least five generations. Flies were cultured in standard fly food and laboratory room temperature (22.5°C). The *"gypsy-TRAP"* transgenic flies were made by cloning a ~500bp Ovo binding site[15] into the NotI site between *Tubulin promoter* and *GAL80* gene in the Tubp-GAL80 in pCaSpeR4 plasmid. The resulting construct was injected into *w1118 (isoCJ1)* recipient embryos and transformant lines were isolated by standard procedures at the BestGene, Inc. The mutated *"gypsy-TRAP"* transgenic flies were made by injecting a similar construct bearing mutations in Ovo binding sites[15]. The *MB247*, *Repo* and *Elav - Gal4* lines are as reported previously [22].

Behavioral Assays

Aversive Pavlovian olfactory task was performed by training flies in a T-maze apparatus using a Pavlovian conditioning paradigm. Approximately 50–100 flies were loaded into an electrifiable training grid. For a single training session, flies were exposed sequentially to one odor (the conditioned stimulus, CS+), which was paired with a 60-volt electric shock and then a second odor (the unconditioned stimulus, CS−) without shock. 2 minutes after this training session, the flies were tested and allowed to choose between the two odors. A

half performance index was calculated by dividing the number of flies that chose correctly, minus the flies that chose incorrectly by the total number of flies in the experiment. The same protocol was then performed with another group of 50–100 flies and reciprocal odor presentation. The final PI was calculated by averaging both reciprocal half PIs. The long-term-memory (LTM) experiment was an adaptation of this training protocol. Flies were subjected to ten such training sessions in robotic trainers spaced out with a 15-minute rest interval between each. Flies then were transferred into food vials and incubated at 18 °C until being tested 24 hours after the training. All genotypes were trained and tested in parallel, and rotated between all the robotic trainers to ensure a balanced experiment. Odor pairs and concentrations used for these behavior paradigms are: 3-Octanol (1.5×10^{-3} v/v) and 4-Methylcyclohexanol (1×10^{-3} v/v), or, 3-Octanol (1.5×10^{-3} v/v) and Benzaldehyde (0.5×10^{-3} v/v). Pure odors were purchased from Sigma and delivered as the stated concentrations with air flow at 750ml/min. In all cases, behavior experiments within a figure were performed in parallel. Behavioral data are normally distributed and are shown as means ± SEM. One-Way ANOVA and post-hoc analyses were performed.

Lifespan

Lifespan were measured with ~50–150 animals/genotype. Equal numbers of male and female flies were used for each genotype. Survival analyses were performed with the Kaplan-Meier Method. Log-rank test and Gehan-Breslow-Wilcoxon test were used to compare survival curves. Pair-wise comparisons were made with Bonferroni corrections.

QPCR

The QPCR was performed according to the assay manual. In brief, massive numbers of fly heads were collected for each genotype and total RNA was purified with Trizol (Invitrogen) and treated by DNaseI (Promega). Total RNA concentrations were determined using a NanoDrop ND-1000 spectrophotometer. For the reverse transcription (RT) reaction, each 20μl RT reaction was performed with 2μg total RNA using the High capacity RNA-to-cDNA kit (Applied Biosystems). The QPCR reactions for each assay were carried out in duplicate, and each 20μl reaction mixture included 1μl previous RT products. The QPCR reaction was carried out and analyzed in an Applied Biosystems 7900HT Fast Real-Time PCR System in 96-well plates at 95°C for 10 min, followed by 40 cycles of 95°C for 15 sec and 60°C for 1 min. Linearity tests were performed on all custom designed primers and probes to ensure linearity.

Custom TaqMan Probes

All TaqMan® Gene Expression Assays (Applied Biosystems) utilized the FAM Reporter and MGB Quencher. TaqMan® probes for each transcript were designed following the vendor's custom assay design service manual. The customized gene-specific Taqman probes and inventoried Taqman probes had the following sequences and Assay IDs.

R1-ORF2 (Assay ID AID1TD0, FBgn0003908):

probe: 5′-ACATACGCCATAATCTG-3′

Blood-ORF2 (assay ID AIFARJ8, FBgn0000199)

Probe: 5′-TCGGTGCATAACTTAGTTAGTTCA-3′

GypsyORF2 (Assay ID AI5IO6V, FBgn0001167)

Probe: 5′-AAGCATTTGTGTTTGATTTC-3′

Gypsy4-ORF2 (AID1TGU, FBgn0063433)

Probe: 5′-CCCGATCTGGGTTGTC-3′

ZAM-ORF2 (Assay IDAICSVAM, FBgn0023131)

Probe: 5′-CCCCATGATTAGTCTTTACTG-3′

1731-ORF2 (Assay ID AICSU7S, FBgn0000007)

Probe: 5′-AAGCTGAAGACTGATTTATG-3′

297-ORF2 (Assay ID AI70LJB, FBgn0000005)

Probe: 5′-TTGATCAAACATACAAATTAATTAC-3′

R25′ (Assay ID AJ0IV12, FBgn0003909)

Probe: 5′-GAATGCCATTCCAAATGGAGAGCCC-3′

R23′ (Assay ID AJY9XVU, FBgn0003909)

Probe: 5′-TAGAAAAATATTGGGCGAACAAGTT-3′

DBV (Assay ID AIV13YJ)

Probe: 5′-CCTATTAGTGATCCGCTCGCG-3′

DTRV (Assay ID AIS07L3)

Probe: 5′-CTTCGATCCGAGGTATGC-3′

DAV (Assay ID AIX00AZ)

Probe: 5′-AAGGTAGTAGGTTACATTTGTC-3′

Sigma V (Assay ID AIWR14R)

Probe: 5′-CCGTAGTCCGATGGTTCC-3′

Nora V (Assay ID AIQJA9N)

Probe: 5′-CTGAGGCTTCTCTTGTTTAAT-3′

DCV (Assay ID AIPAC3F)

Probe: 5′-TTGTCGACGCAATTCTT-3′

DXV (Assay ID AIRR9FV)

Probe: 5′-TCATAGATGATGTCAAATTT-3′

ANV (Assay ID AIT95SB)

Probe: 5′-CAGACAATTTCTCAGAATCAT-3′

Act5C (Assay ID Dm02361909_s1)

Loki (Assay ID Dm01811114_g1)

Ago2 (Assay ID Dm01805432_g1 and Dm01805433_g1)

Dcr-2 (Assay ID Dm01821537_g1 and Dm01821540_g1)

Western Blots

~15 adult fly heads per sample were homogenized in 20ul Nupage@ sample loading buffer, heated to 95 °C for 5 min and 10 μl loaded onto Nupage@ 4–12% Bis-Tris gels, then transferred to PVDF membrane (Invitrogen) and blotted by standard protocols. Primary antibodies used were anti-tubulin (1:10,000, E7, Developmental Studies Hybridoma Bank), anti-ENV (1:5000). The WesternBreeze® Chemiluminescent Kit–Anti-Mouse system was used to visualize the blotted bands on films.

Bleach Treatment of Embryos

In order to remove virus infection in fly stocks, 2hr embryos from wild type controls and *dAgo2* mutants were collected and treated with 50% bleach 2 times for 20 minutes each. Treated embryos were then grown in a virus free clean room equipped with UV lamps to sterilize surfaces. Expanded fly stocks after bleach treatment are proven to be virus-free. All strains also were grown on a rotating set of 6 antibiotics.

Immunohistochemistry and GFP Imaging

Dissection, fixation, immunolabeling and confocal imaging acquisition were performed as previously described[23]. Ascites containing anti-gypsy ENV monoclonal antibody (mAb) was prepared from the anti-gypsy ENV 7B3 hybridoma cell line[24]. A 1:100 dilution of ENV primary mAb and a 1: 200 dilution of secondary antibody of Cy3-conjugated goat anti-mouse IgG were used. We used 2μM DilC18(5)-DS lipophilic dye solution (Molecular Probes) to label cell membranes throughout the brain as counterstaining. For Env immunolabeling, we imaged multiple brains of each genotype and age. Representative images are shown in figures. Totals numbers imaged for wild type were: 6 (0–4day), 14 (14day), 16 (21–28 day), 4 (70 day). For $dAgo2^{414}$, total number imaged were: 8 (14 day), 7 (21–28 day). For dAgo2-51b, total number imaged were: 5 (0–4 day), 6 (14 day), 6 (21–28

day), 3 (70 day). For *dAgo2*^{454}, total number imaged were 9 (0–4 day), 13 (14 day), 6 (21–28 day).

Nested PCR

DNA was extracted from ~300 fly heads of the indicated ages. Standard PCR was preformed in nested fashion with the first round of PCR utilizing primer 1 and 3 followed by a second round of pcr with primer 2 and 4. Primer sequences are listed below. Nested PCR was then run on .9% agarose gel (Sigma) and size was estimated according to 1 kb plus DNA ladder (Invitrogen). The PCR product was then gel purified using illustra GFX PCR DNA and Gel Band Purification Kit from GE Healthcare. The fragment was cloned using the TOPO TA Cloning Kit for sequencing from Invitrogen and sequenced by ELIM BIOPHARM using the Sanger sequencing method. MacVector was used to display sequencing results.

Primers

Primer 1 - CAACTCTGCACCCACGACTA

Primer 3 - CAGCGGAAAGCTGACACTTC

Primer 2 - CACACACCCATGGAATTGAA

Primer 4 - GGCTCATTGCCGTTAAACAT

Statistical Testing

Behavioral data from the Pavlovian memory task are normally distributed [21] and are shown in all figures as means ± SEM. For these data, one-Way ANOVA and post-hoc analyses were performed. For the life-span curves, survival analyses were performed with the Kaplan-Meier Method. Log-rank test and Gehan-Breslow-Wilcoxon test were used to compare survival curves. Pair-wise comparisons were made with Bonferroni corrections.

Supplementary Material

Refer to Web version on PubMed Central for supplementary material.

Acknowledgments

We thank Benjamin Czech and Gregory Hannon for the *dAgo2*^{414} and *lokiRNAi* fly line, Fen-Biao Gao for the *dAgo2*^{51B} fly line, Barry Dickson for the *UAS::dAgo2* transgenic fly line, Michael Welte for the *dAgo2*^{454} fly line, Tzumin Lee for the pTub-GAL80 in Casper4 plasmid, Jeff Boek for the 7B3 hybridoma cell line and Carmelita Bautista at the CSHL shared resources for ascites production. We also are grateful to Scott Waddell, Jennifer Beshel, Michael Cressy, Benjamin Czech, Gregory Hannon, Kyle Honegger, Josh Huang, Maurice Kernan, Rob Martienssen, Hongtao Qin, Carmen Sandoval, Yichun Shuai, Glenn Turner, Tony Zador and Yi Zhong for helpful discussions or comments on the manuscript. This work was supported by NIH TR01(5R01NS067690-03) and DART neuroscience LLC awarded to JD. SG received additional support from the Shakespeare Fellowship and the Ernst Göhner Foundation.

References

1. Belancio VP, Hedges DJ, Deininger P. Genome Res. 2008; 18:343–358.10.1101/gr.5558208 [PubMed: 18256243]

2. Goodier JL, Kazazian HH Jr. Cell. 2008; 135:23–35.10.1016/j.cell.2008.09.022 [PubMed: 18854152]
3. Muotri AR, et al. Nature. 2005; 435:903–910.10.1038/nature03663 [PubMed: 15959507]
4. Coufal NG, et al. Nature. 2009; 460:1127–1131.10.1038/nature08248 [PubMed: 19657334]
5. Baillie JK, et al. Nature. 2011; 479:534–537.10.1038/nature10531 [PubMed: 22037309]
6. Lathe R, Harris A. J Mol Biol. 2009; 392:813–822.10.1016/j.jmb.2009.07.045 [PubMed: 19631225]
7. Muotri AR, et al. Nature. 2010; 468:443–446.10.1038/nature09544 [PubMed: 21085180]
8. Jeong BH, Lee YJ, Carp RI, Kim YS. J Clin Virol. 2010; 47:136–142.10.1016/j.jcv.2009.11.016 [PubMed: 20005155]
9. Coufal NG, et al. Proc Natl Acad Sci U S A. 2011; 108:20382–20387.10.1073/pnas.1100273108 [PubMed: 22159035]
10. Douville R, Liu J, Rothstein J, Nath A. Ann Neurol. 2011; 69:141–151.10.1002/ana.22149 [PubMed: 21280084]
11. Kaneko H, et al. Nature. 2011; 471:325–330.10.1038/nature09830 [PubMed: 21297615]
12. Tan H, et al. Hum Mol Genet. 2012; 21:57–65.10.1093/hmg/ddr437 [PubMed: 21940752]
13. Li W, Jin Y, Prazak L, Hammell M, Dubnau J. PLoS One. 2012; 7:e44099.10.1371/journal.pone.0044099 [PubMed: 22957047]
14. Czech B, Hannon GJ. Nat Rev Genet. 2011; 12:19–31.10.1038/nrg2916 [PubMed: 21116305]
15. Labrador M, Sha K, Li A, Corces VG. Genetics. 2008; 180:1367–1378.10.1534/genetics.108.094318 [PubMed: 18791225]
16. Schwaerzel M, Heisenberg M, Zars T. Neuron. 2002; 35:951–960. [PubMed: 12372288]
17. Dubnau J, Chiang AS. Curr Opin Neurobiol. 201210.1016/j.conb.2012.09.006
18. Lim DH, et al. FEBS Lett. 2011; 585:3079–3085.10.1016/j.febslet.2011.08.034 [PubMed: 21889502]
19. Liu N, et al. Nature. 2012; 482:519–523.10.1038/nature10810 [PubMed: 22343898]
20. Chen Y, Pane A, Schupbach T. Curr Biol. 2007; 17:637–642.10.1016/j.cub.2007.02.027 [PubMed: 17363252]
21. Tully T, Preat T, Boynton SC, Del Vecchio M. Cell. 1994; 79:35–47. [PubMed: 7923375]
22. Qin H, et al. Curr Biol. 2012; 22:608–614.10.1016/j.cub.2012.02.014 [PubMed: 22425153]
23. Chen G, et al. PLoS Comput Biol. 2008; 4:e1000026.10.1371/journal.pcbi.1000026 [PubMed: 18463699]
24. Song SU, Gerasimova T, Kurkulos M, Boeke JD, Corces VG. Genes Dev. 1994; 8:2046–2057. [PubMed: 7958877]

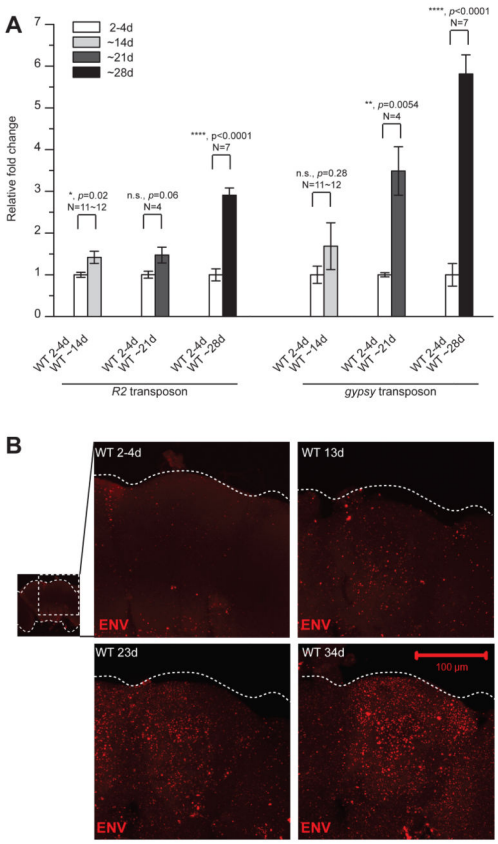

Figure 1. Age dependent increases in expression of LINE-like and LTR retrotransposons in *Drosophila* brain

(**A**) Levels of transcripts of *R2* and *gypsy* quantified by QPCR from young (2–4-day) and aged (~14-day, ~21-day and ~28-day) wild type (WT) heads. Transcript levels normalized to *Actin and* shown as fold changes relative to WT (means ± SEM). (**B**) ENV immunofluorescence is elevated in brains from older animals (13-day, 23-day, 34-day) relative to ~2–4-day old animals. Projection through the central brain are shown. ENV signal is detected throughout the cortex layer that includes most of the cell bodies as well as in neuropil areas of axons and dendrites (see also individual confocal sections in Figs. 3B and S5B).

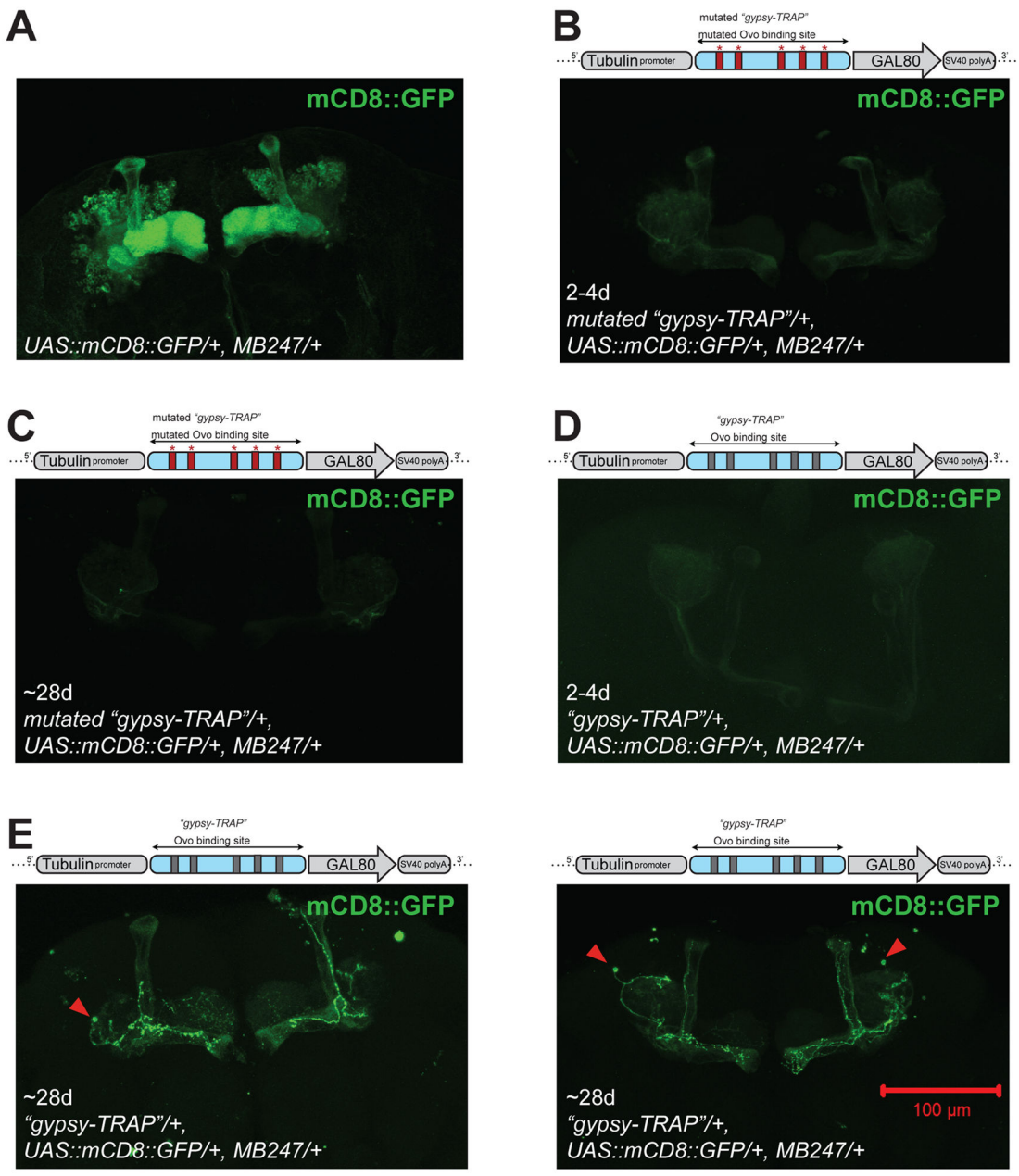

Figure 2. *"Gypsy-TRAP"* reporter detects *de novo* integration in neurons in aged animals

A ~500bp fragment from the *ovo* regulatory region containing 5 Ovo binding sites is inserted between *Tub promoter* and *GAL80* gene. A mutated *"gypsy-TRAP"* construct contains mutations that disrupt each of the 5 Ovo binding sites. In the absence of *gypsy* insertions, GAL80 expression suppresses GAL4, and *UAS::mCD8::GFP* is not expressed. In the presence of *gypsy* integration into the *"gypsy-TRAP"*, GAL80 expression is blocked, and *UAS::mCD8::GFP* is turned on (see Fig. S2). (**A**) Approximately 800 mushroom body Kenyon cell neurons per brain hemisphere are labeled by *MB247-GAL4*-driven *U*AS::mCD8::GFP. (**B**) An example brain from 2–4-day old mutated *"gypsy-TRAP"; UAS::mCD8::GFP/+; MB247/+*. No GFP labeled neurons seen. (**C**) An example brain from

~28-day old mutated *"gypsy-TRAP";UAS::mCD8::GFP/+; MB247/+*. No GFP labeled neurons seen. (**D**) An example brain from ~2–4-day old *"gypsy-TRAP"; UAS::mCD8::GFP/+; MB247/+*. No GFP labeled neurons seen. (**E**) Example brains from ~28-day old *"gypsy-TRAP"; UAS::mCD8::GFP/+; MB247/+*. Several GFP-labeled MB neurons seen in each brain. See Table S1 and Fig. S2 for statistical summary and additional example images.

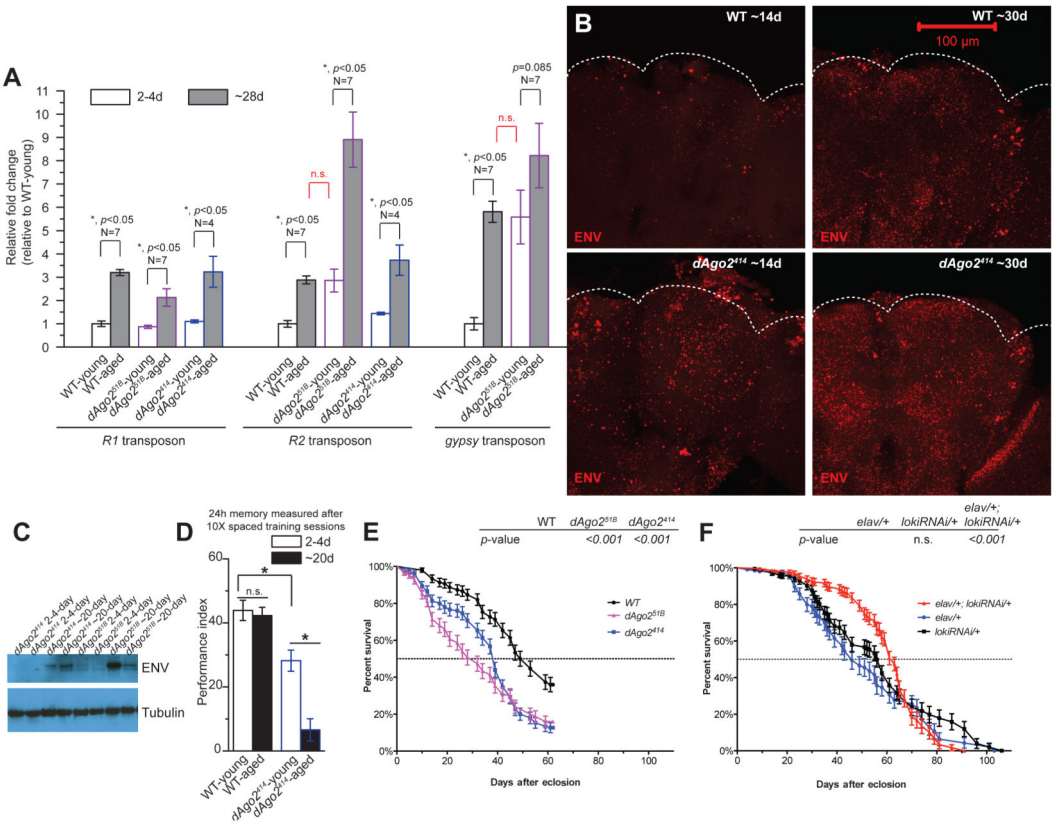

Figure 3. Age-dependent TE expression contributes to memory decline and age-dependent mortality

(**A**) Levels of transcripts of *R1*, *R2* and *gypsy* were quantified from young (2–4-day) and aged (~28-day) WT and *dAgo2* mutant animal heads. Within all genotypes, aged animals have significantly elevated levels of each of the transposon transcripts (*R1*, *R2*, and *gypsy*), compared to young animals (*, $p<0.05$, N=4 for both young and aged $dAgo2^{414}$ groups, N=7 for both young and aged WT and $dAgo2^{51B}$ groups), except for the comparison between young and aged groups within $dAgo2^{51B}$ ($p=0.085$) for *gypsy*, which also is elevated in young animals. For *R2* and *gypsy*, transcript levels in $dAgo2^{51B}$ young groups are as high as in WT aged groups. ~28-day old $dAgo2^{51B}$ animals exhibit dramatically increased levels of *R2* compared to aged WT group (*, $p<0.05$). For R2, the 5′ probe set was used in this experiment (see Online Methods) (**B**) ENV immunoreactivity is detected throughout the cortex layer that includes most of the somata as well as in neuropil (see also Figs. 1 and S5B). Central projections are shown for whole mount brains. Brains from $dAgo2^{414}$ mutants exhibit higher levels of ENV immunolabeling in ~14-day old and ~30-day old animals, as also is observed with other *dAgo2* alleles (Fig. S5B). (**C**) Western blot detection with ENV monoclonal antibody shows age-dependent accumulation in heads from *dAgo2* mutant animals (see also Fig. S5A). Levels for $dAgo2^{51B}$ appear increased although somewhat variable. (**D**) LTM performance (means ± SEM) shown for 2–4-day old and ~20-day old WT and $dAgo2^{414}$ mutant animals. 2–4-day old $dAgo2^{414}$ mutants exhibit significantly reduced LTM performance relative to 2–4-day old WT animals, and show a dramatic further reduction in performance in the 20-day old $dAgo2^{414}$ mutant group (*, $p<0.05$ and N=15).

(**E**) Lifespan is significantly shortened for *dAgo2*^{414} and *dAgo2*^{51B} animals relative to WT (log-rank test). (**F**) Knocking down *loki* gene expression with *lokiRNAi* in neurons significant delays mortality (Gehan-Breslow-Wilcoxon test) of the *elav/+; lokiRNAi/+* animals compared to heterozygous controls for transgenes (*elav/+* and *lokiRNAi/+*), as well as the onset of age-dependent memory decline (Fig. S7).